Short-wavelength InAlGaAs/AlGaAs quantum dot superluminescent diodes*

Liang De-Chun(梁德春), An Qi(安 琪), Jin Peng(金 鹏)†, Li Xin-Kun(李新坤), Wei Heng(魏 恒), Wu Ju(吴 巨), and Wang Zhan-Guo(王占国)

Key Laboratory of Semiconductor Materials Science, Institute of Semiconductors, Chinese Academy of Sciences, Beijing 100083, *China*

(Received 24 March 2011; revised manuscript received 9 May 2011)

This paper reports the fabrication of J-shaped bent-waveguide superluminescent diodes utilizing an InAlGaAs/AlGaAs quantum dot active region. The emission spectrum of the device is centred at 884 nm with a full width at half maximum of 37 nm and an output power of 18 mW. By incorporating an Al composition into the quantum dot active region, short-wavelength superluminescent diode devices can be obtained. An intersection was found for the light power-injection current curves measured from the straight-waveguide facet and the bent-waveguide facet, respectively. The result is attributed to the conjunct effects of the gain and the additional loss of the bent waveguide. A numerical simulation is performed to verify the qualitative explanation. It is shown that bent waveguide loss is an important factor that affects the output power of J-shaped superluminescent diode devices.

Keywords: InAlGaAs quantum dot, superluminescent diode, optical coherence tomography, short wavelength

PACS: 85.60.Jb, 78.67.Hc, 81.07.Ta, 81.16.Dn **DOI:** 10.1088/1674-1056/20/10/108503

1. Introduction

Optical coherence tomography (OCT),[1,2] a new technology for medical diagnostics, has been successfully developed during the past decade as a high-spatial-resolution imaging method *in vivo*. High brightness and low coherence are the main requirements of the light source for an OCT system.[3] For a light source with a Gaussian spectral line shape, its coherence length is determined by $L_{\rm coh} = \lambda_m^2/\Delta\lambda$, where λ_m is the central wavelength of the spectrum and $\Delta\lambda$ is the full width at half maximum (FWHM). The theoretical axial resolution for an OCT system, ΔL, is in proportion to the coherence length of the light source used, $\Delta L \propto L_{\rm coh}$.[4] So a light source with a short wavelength and a large FWHM is preferred for OCT applications. Until now, superluminescent diodes (SLDs) with a central wavelength in the 800 nm–950 nm range, which belong to the short-wavelength near-infrared band, are the most commonly used sources in ophthalmic OCT systems because of their short coherence length and transparency in ocular lens and liquid.

It has been proposed and proved that the size inhomogeneity naturally occurring in self-assembled quantum dots (QDs)[5,6] grown by the Stranski–Krastanow mode is beneficial to broadband emitting devices, such as SLDs[7−10] and tunable external-cavity lasers.[11−14] Broadband and/or high-power QD-SLDs have been developed.[15] Very recently, a 1.3-μm high-power and broadband QD-SLD has been used in an OCT system and successful skin imaging has been demonstrated.[16,17]

GaAs and InP-based In(Ga)As QDs are now widely used for fabricating broadband SLDs emitting wavelengths longer than 900 nm. However, it is difficult for In(Ga)As QDs to obtain shorter emission wavelengths. It has been demonstrated by some groups that $In_xAl_yGa_{1-x-y}As$ QDs are suitable for light emitting shorter than 900 nm.[18,19] One can tune the emission wavelength by changing the composition of the $In_xAl_yGa_{1-x-y}As$ QDs easily. Recently, $In_xAl_yGa_{1-x-y}As$ QDs have been successfully used to fabricate laser devices with a lasing wavelength in the 760 nm–920 nm range. But SLDs have not profited from the advantages of $In_xAl_yGa_{1-x-y}As$ QDs until

*Project supported by the National Basic Research Program of China (Grant No. 2006CB604904) and the National Natural Science Foundation of China (Grant Nos. 60876086, 60976057, and 60776037).

†Corresponding author. E-mail: pengjin@red.semi.ac.cn

© 2011 Chinese Physical Society and IOP Publishing Ltd

now.

In this paper, GaAs-based short-wavelength SLDs with InAlGaAs/AlGaAs QDs as the active region are demonstrated. Both the J-shaped bent-waveguide (BW) structure and facet anti-reflection (AR) coating are used to suppress lasing. The devices are characterized by their power and emission spectrum measurements. An SLD device with a 37-nm FWHM and 18-mW light power was obtained. A numerical calculation is done to simulate the light power–injection current (P–I) property of the SLD devices.

2. Experiment

The InAlGaAs/AlGaAs QD epitaxial structure was grown by a Riber 32P solid source molecular beam epitaxy (MBE) system on an n-GaAs (100) substrate tilted toward (111)A by 4°. It is a typical separate confinement heterostructure and the active region consists of ten layers of 5.4 monolayer $In_{0.45}Al_{0.2}Ga_{0.35}As$ QDs in the $Al_{0.25}Ga_{0.75}As$ matrix. Each QD's active region is embedded in a 100-nm thick $Al_{0.25}Ga_{0.75}As$ waveguide layer. Below and above the waveguide are 1.5-μm-thick n-type and 1.5-μm-thick p-type $Al_{0.5}Ga_{0.5}As$ cladding layers, respectively. Finally, a 250-nm thick p^+-GaAs layer was capped as the Ohmic contact layer. The substrate temperature was 700 °C for all the AlGaAs layers and was 560 °C for the InAlGaAs QD layers during MBE growth. In order to investigate the morphology of the $In_{0.45}Al_{0.2}Ga_{0.35}As/Al_{0.25}Ga_{0.75}As$ QDs, an uncapped single-layer QD reference sample was grown with the same growth conditions as that of the device structure. Then the QD device wafer was processed to fabricate SLD devices with J-shaped BW structures.[21] The main structural parameters are shown in Fig. 3. The final devices have a 20-μm-wide ridge waveguide and a 3.5-mm-long cavity with a 1-mm bent part. The curvature radius of the BW is 8.2 mm, resulting in about 7° tilting from the normal direction of the cleaved facet. The devices were mounted epitaxial-side down on copper heat sinks. For a portion of the devices, a single $\lambda/4$ SiO_2 AR layer designed for minimum reflectivity at about 900 nm was deposited on the BW facet, while the straight-waveguide (SW) facet remained as-cleaved. The devices were characterized by P–I and electroluminescence (EL) measurements at room temperature in pulsing injection mode with a repetition rate and duty cycle of 1 kHz and 3%, respectively. The power value is presented as the peak power, which is deduced from the average one measured with a pyroelectric probe divided by the 3% duty cycle.

3. Results and discussion

Figure 1 shows a photoluminescence (PL) spectrum measured at 5.5 K of the InAlGaAs QD-SLD device epitaxial structure, whose central wavelength is around 860 nm with an FWHM of 85 nm. A typical atomic force microscope (AFM) image of the uncapped reference sample is shown in the inset of Fig. 1. A statistic gives a result that the QD material has a sheet density of 4.7×10^{10} cm^{-2}, an average height of 4.9 nm and an average width of 38 nm.

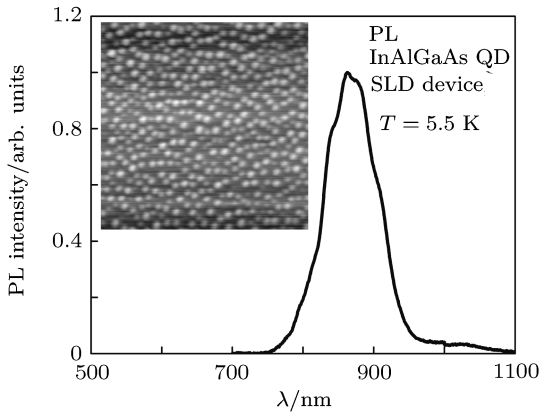


Fig. 1. Low-temperature PL spectrum of the InAlGaAs/AlGaAs QD SLD device structure. The inset shows an AFM image (1 μm×1 μm) of the InAlGaAs/AlGaAs QD reference sample.

In order to check the performance of the device wafer, laser diodes (LDs) have been fabricated. A P–I curve and the emitting spectra of a QD-LD with 2-mm cavity length and 20-μm ridge width are presented in Fig. 2. The $(0\bar{1}1)$ facets were used for the optical feedback to fabricate a Fabry–Pérot cavity. The threshold current of the device is 0.7 A (1.75 kA/cm^2 threshold current density). The threshold current density of the InAlGaAs/AlGaAs QD laser is higher than that of the InAs/GaAs QD devices.[22] This may be related to defects within the InAlGaAs QD active region. The introduction of aluminum in the active region, which is sensitive to oxygen-related background species (e.g., O_2, H_2O, CO, and CO_2), may induce large numbers of defects, resulting in considerable non-radiation

recombination.[23] The inset of Fig. 2 shows the emitting spectra of the QD laser under various injection levels above the threshold. The lasing emission wavelength is centred at around 906 nm. It can be seen from Fig. 2 that with increasing the injection current, the FWHM increased for the emission spectra of the laser. This was related to the inhomogeneous size distribution of the self-assembled QDs.

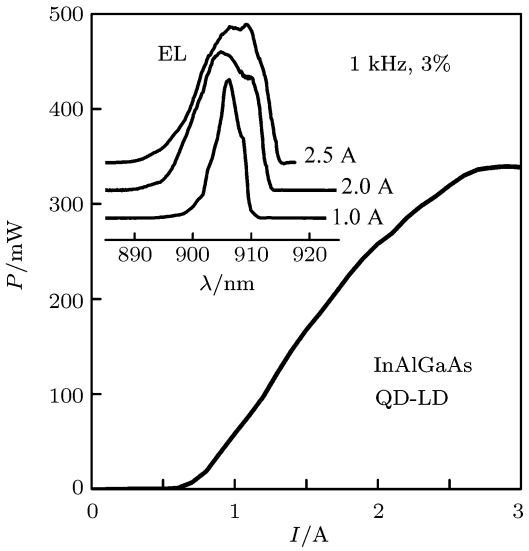


Fig. 2. The P–I curve of an InAlGaAs/AlGaAs QD laser diode in pulsed injection mode at room temperature. The inset shows EL spectra of the QD laser under various injection levels.

Figure 3 shows the P–I property of an InAlGaAs QD-SLD measured from the BW and SW facets, respectively, exhibiting typical superluminescent behaviour, especially for the BW facet. The output power is 18 mW under 5-A injection current. A far-field pattern measured from the BW facet is given in the inset of Fig. 3, which shows a crescent-shaped profile because of the curved waveguide.[21] No lasing is found even when the injection current is up to 5 A, as demonstrated in the emission spectrum in Fig. 4, which is centred at 884 nm with the FWHM of 37 nm.

Due to the difference in retro-reflectivity between the two facets, the J-shaped SLD device always emits a higher power from the BW facet than that of the SW facet. As a result, the BW facet is usually used in devices as the power output facet. For the BW facet, the retro-reflectivity is smaller because of the curved waveguide and the AR coating. The retro-reflectivity of the SW facet is relatively large (∼30%) as the facet remains as-cleaved. Therefore, under the injection level that the superluminescence occurs, light emitted from the BW facet can experience double-path amplification while the light emitted from the SW facet can only experience single-path amplification.[21] As a result, a typical soft-threshold character is observed for the P–I curve measured from the BW side.

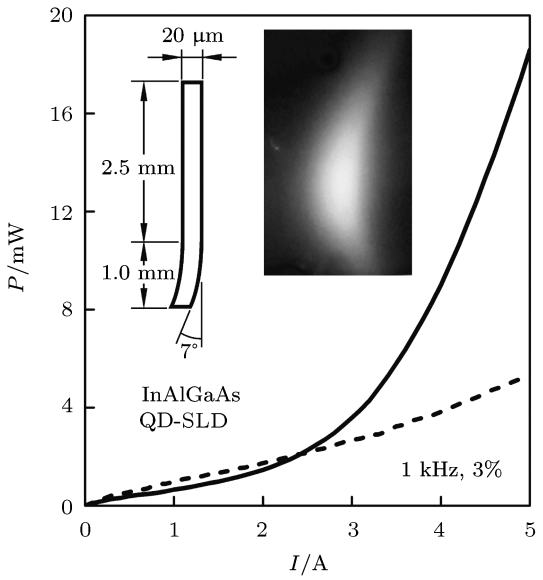


Fig. 3. The P–I curves of an InAlGaAs/AlGaAs QD-SLD device measured from the BW facet (solid line) and the SW facet (dashed line). The insets show the schematic diagram of the device structure (left) and the far-field pattern taken from the BW facet (right, 4.5-A injection current).

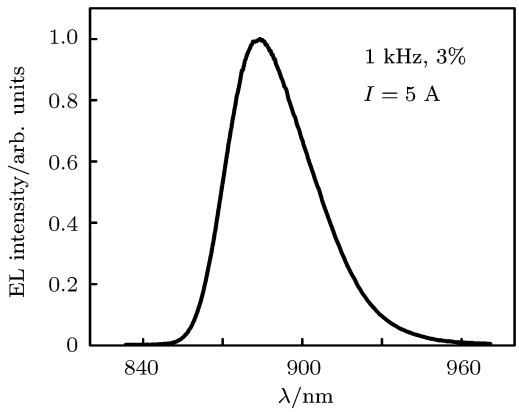


Fig. 4. Normalized EL spectrum of an InAlGaAs/AlGaAs QD-SLD under 5-A injection current measured from the BW facet.

Figure 3 shows the P–I curves of an InAlGaAs/AlGaAs QD-SLD device measured from both the BW facet (solid line) and the SW facet (dashed line); it can be seen from the figure that the two curves intersect at 2.4 A. The light power from the BW facet is higher than that from the SW facet when the injection current is more than 2.4 A; while for the current less than 2.4 A, the power for the BW facet is slightly

lower. We attribute this phenomenon to the conjunct effects of the gain and the curved waveguide loss. When the injection current is small enough, spontaneous radiation dominates the light emission from the device. Then the larger loss of the curved waveguide leads to a lower output power from the BW facet. When increasing the injection current to make the superluminescence dominate the light emission process, the double-path gain counteracts the additional curved waveguide loss and makes the light power from the BW facet higher. A single-path gain leads to less power from the SW facet.

A simple numerical simulation has been performed to verify the above qualitative explanation. In the simulation, besides the same internal waveguide loss $\alpha_{\rm i}$ as the SW part, the BW part has additional loss $\alpha_{\rm b}$ because of its curved shape. Figure 5 shows the simulated P–I curves with different BW loss $\alpha_{\rm b}$ and the same internal waveguide loss $\alpha_{\rm i}$ of 1.5 cm^{-1}. For small BW loss $\alpha_{\rm b}$ = 5 cm^{-1}, as shown in Fig. 5(a), light power from the BW facet is higher than that from the SW facet throughout the current range. For both the mid BW losses $\alpha_{\rm b}$ = 22 cm^{-1} and 30 cm^{-1}, as shown in Figs. 5(b) and 5(c), intersections between the two curves in the figures occur. When increasing the BW loss $\alpha_{\rm b}$ further, as shown in Fig. 5(d), no intersection is found in the current range from 0 A to 5 A. Power from the BW facet is lower than that from the SW facet throughout the current range. It is shown in Fig. 5 that the P–I curves from the SW facet have little dependence on the BW loss $\alpha_{\rm b}$. However, BW loss $\alpha_{\rm b}$ affects the light output properties of the BW facet observably. A larger BW loss means a lower output power emitting from the BW facet. So the BW loss is an important factor that affects the output power of the J-shaped SLD devices. Detailed description of the simulation and its further numerical results regarding J-shaped waveguide QD-SLD devices will be presented elsewhere.

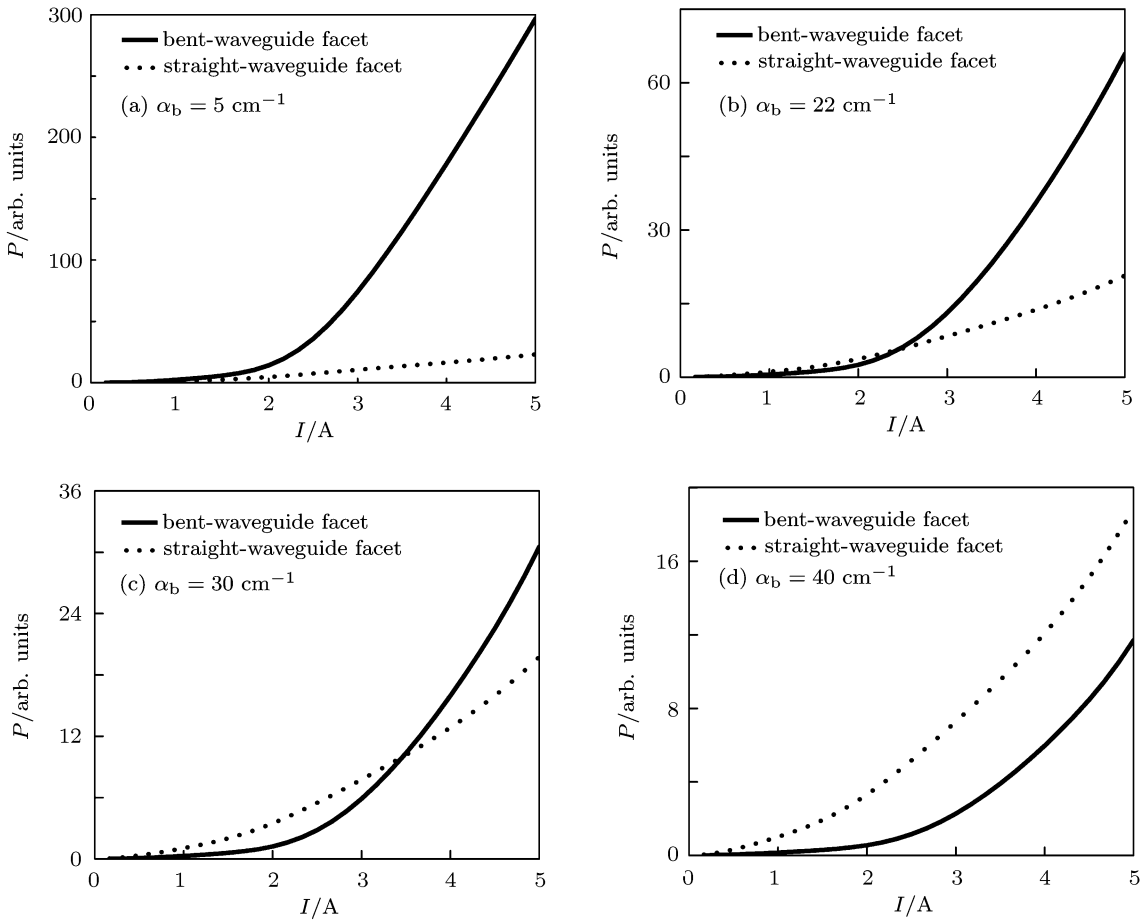


Fig. 5. Numerically simulated P–I curves from the BW facet (solid lines) and the SW facet (dashed lines) respectively with the BW loss $\alpha_{\rm b}$ of (a) 5 cm^{-1}, (b) 22 cm^{-1}, (c) 30 cm^{-1}, and (d) 40 cm^{-1}.

4. Conclusion

GaAs-based short-wavelength SLDs with an InAlGaAs/AlGaAs quantum dot active region have been demonstrated. An emission spectrum centred at 884 nm was obtained with a 37-nm FWHM and 18-mW light power under 5-A injection current. An intersection was found for the two P–I curves measured from the SW waveguide and BW facets, respectively. We attribute the result to the conjunct effects of the gain and the additional loss of the BW. The qualitative explanation was verified by a numerical simulation. It is shown that the BW loss is an important factor that affects the output power of J-shaped SLD devices.

References

[1] Hee M R, Izatt J A, Swanson E A, Huang D, Schuman J S, Lin C P, Puliafito C A and Fujimoto J G 1995 *IEEE Eng. Med. Biol.* **14** 67

[2] Wang K, Zeng Y, Ding Z H, Meng J, Shi G H and Zhang Y D 2010 *Acta Phys. Sin.* **59** 2471 (in Chinese)

[3] Liang Y M, Zhou D C, Meng F Y and Wang M W 2007 *Acta Phys. Sin.* **56** 3246 (in Chinese)

[4] Brezinski M E and Fujimoto J G 1999 *IEEE J. Sel. Topics Quantum Electron.* **5** 1185

[5] Dou X M, Sun B Q, Huang S S, Ni H Q, Niu Z C, Yang F H and Jia R 2009 *Chin. Phys.* B **18** 2258

[6] Li Y, Dou X M, Chang X Y, Ni H Q, Niu Z C and Sun B Q 2011 *Acta Phys. Sin.* **60** 017804 (in Chinese)

[7] Sun Z Z, Ding D, Gong Q, Zhou W, Xu B and Wang Z G 1999 *Opt. Quantum Electron.* **31** 1235

[8] Zhang Z Y, Wang Z G, Xu B, Jin P, Sun Z Z and Liu F Q 2004 *IEEE Photon. Technol. Lett.* **16** 27

[9] Liu N, Jin P and Wang Z G 2005 *Electron. Lett.* **41** 1400

[10] Lü X Q, Liu N, Jin P and Wang Z G 2008 *IEEE Photon. Technol. Lett.* **20** 1742

[11] Lü X Q, Jin P, Wang W Y and Wang Z G 2010 *Opt. Express* **18** 8916

[12] Lü X Q, Jin P and Wang Z G 2010 *Chin. Phys.* B **19** 018104

[13] Wu J, Lü X Q, Jin P, Meng X Q and Wang Z G 2011 *Chin. Phys.* B **20** 064202

[14] Fedorova K A, Cataluna M A, Krestnikov I, Livshits D and Rafailov E U 2010 *Opt. Express* **18** 19438

[15] Zhang Z Y, Hogg R A, Lü X Q and Wang Z G 2010 *Adv. Opt. Photon.* **2** 201

[16] Krstajić N, Smith L E, Matcher S J, Childs D T D, Bonesi M, Greenwood P D L, Hugues M, Kennedy K, Hopkinson M, Groom K M, MacNeil S, Hogg R A and Smallwood R 2010 *IEEE J. Sel. Topics Quantum Electron.* **16** 748

[17] Greenwood P D L, Childs D T D, Kennedy K, Groom K M, Hugues M, Hopkinson M, Hogg R A, Krstajić N, Smith L E, Matcher S J, Bonesi M, MacNeil S and Smallwood R 2010 *IEEE J. Sel. Topics Quantum Electron.* **16** 1015

[18] Baklenov O, Huffaker D L, Anselm A, Deppe D G and Streetman B G 1997 *J. Appl. Phys.* **82** 6362

[19] Schlereth T W, Schneider C, Höfling S and Forchel A 2008 *Nanotechnology* **19** 045601

[20] Schlereth T W, Schneider C, Gerhard S, Höfling S and Forchel A 2009 *IEEE J. Sel. Topics Quantum Electron.* **15** 792

[21] Lin C F and Juang C S 1996 *IEEE Photon. Technol. Lett.* **8** 206

[22] Ustinov V M, Zhukov A E, Egorov A Yu and Maleev N A 2003 *Quantum Dot Lasers* (New York: Oxford)

[23] Liu H Y, Sellers I R, Airey R J, Steer M J, Houston P A, Mowbray D J, Cockburn J, Skolnick M S, Xu B and Wang Z G 2002 *Appl. Phys. Lett.* **80** 3769